ANL-18/33

Modeling and Simulations of Thermal-Fluid Phenomena Related to Pressurized Conduction Cooldown in High Temperature Gas Reactor

Nuclear Science and Engineering Division

About Argonne National Laboratory

Argonne is a U.S. Department of Energy laboratory managed by UChicago Argonne, LLC under contract DE-AC02-06CH11357. The Laboratory's main facility is outside Chicago, at 9700 South Cass Avenue, Argonne, Illinois 60439. For information about Argonne and its pioneering science and technology programs, see www.anl.gov.

DOCUMENT AVAILABILITY

Online Access: U.S. Department of Energy (DOE) reports produced after 1991 and a growing number of pre-1991 documents are available free via DOE's SciTech Connect (http://www.osti.gov/scitech/)

Reports not in digital format may be purchased by the public from the National Technical Information Service (NTIS):

U.S. Department of Commerce
National Technical Information Service
5301 Shawnee Rd
Alexandra, VA 22312
www.ntis.gov
Phone: (800) 553-NTIS (6847) or (703) 605-6000
Fax: (703) 605-6900
Email: **orders@ntis.gov**

Reports not in digital format are available to DOE and DOE contractors from the Office of Scientific and Technical Information (OSTI):

U.S. Department of Energy
Office of Scientific and Technical Information
P.O. Box 62
Oak Ridge, TN 37831-0062
www.osti.gov
Phone: (865) 576-8401
Fax: (865) 576-5728

ANL-18/33

Modeling and Simulations of Thermal-Fluid Phenomena Related to Pressurized Conduction Cooldown in High Temperature Gas Reactor

prepared by
Prasad Vegendla, Rui Hu, Haomin Yuan
Nuclear Science and Engineering Division, Argonne National Laboratory

September 2018

EXECUTIVE SUMMARY

Under the support of DOE-NE's Nuclear Energy Advanced Modeling and Simulation (NEAMS) Program, an effort is being pursued to support High Temperature Gas Reactors (HTGR) technology development and its modeling and simulation needs. There is a particular need for advanced modeling & simulation tools to predict thermal-fluid behavior in the nuclear reactor primary system—especially the core and lower and upper plena—during safety-related transients. To help accomplish this, we must provide confidence in the reliability and accuracy of the thermal fluid simulation tools being developed under the NEAMS program for HTGR applications. The benchmark simulations of the available experimental tests would help us in this effort.

During a Pressurized Conduction Cooldown (PCC) in an HTGR event where the blower fails, flow in the core and risers transitions from forced downward flow to buoyancy-driven upward flow. This often leads, for some period of time, to significant degradation of heat transfer in the core associated with the transition from turbulent to laminar flow. During the transient, hot plumes from the core channels may impinge on upper plenum structures.

The initial objective of this work was to verify and validate the CFD models for these two phenomena with data for a $1/16^{th}$ scaled Very High Temperature Reactor (VHTR) at Texas A&M University (TAMU), and the Deteriorated Turbulent Heat Transfer (DTHT) in a circular tube (coolant channel) measured at Massachusetts Institute Technology (MIT).

In the TAMU benchmark, fluid enters a lower plenum from a horizontal inlet pipe, splits into several vertical inlet channels, and enters the scaled dome-shaped test section where the jet mixing occurs. In FY17, the CFD simulation campaign focused only on the test section and the vertical inlet channels, assuming that the flow rate in each coolant channel was identical. The results of the Nek5000 and STAR-CCM+ calculations were inconsistent with the measured data, which exhibited asymmetry that neither code could predict for multi-jet flows. In FY18, the jet flow characteristics were investigated in two different upper plenum configurations; (i) single coolant channel and (ii) multiple (five) coolant channel. First, CFD models were verified with two different codes, Nek5000 and STAR-CCM+, for the single coolant channel configuration. The predicted jet velocities were identical in both codes with a marginal deviation due to differences in turbulence modeling. Second, the STAR-CCM+ Reynolds Stress Model (RSM) was validated with a multiple coolant channel configuration. Good agreement between simulated results and measured data was obtained for jet peak velocities. Also, the predicted flow asymmetry was similar to experimental data. In contrast, significant deviations were observed in the off side peak velocities due to the assumption of a constant inlet mass flow rate.

In the DTHT benchmark, non-isothermal modeling and simulations were performed for a wall heated circular tube. The simulation results were verified with two different CFD tools, Nek5000 and STAR-CCM+, and validated with experimental data. The predicted bulk temperatures were identical in both CFD tools, as expected. Good agreement between simulated results and measured data were obtained for wall temperatures along the tube axis using Nek5000. In STAR-CCM+, the under-predicted wall temperatures were due to higher turbulence in the wall region.

Future work will include analyzing the modular HTGR domain during PCC event and developing the heat transfer correlations for natural circulation regime using Nek5000. In the PCC event, the Reynolds numbers can approach as low as ~500 during the development of a natural circulation flow from a forced circulation flow. The high-fidelity CFD tool can help to guide the low-order models to accomplish the plant-level simulations, efficiently and accurately. This effort includes collecting heat transfer correlations from literature and verifying with the Nek5000 results for various Reynolds flows (50 to 2000) and wall heat fluxes (1000 to 20000 W/m^2). The ultimate goal of this project is to develop a computationally efficient capability that attempts to predict flow and heat transfer in the core and plena during the transient events. To achieve this, we plan to integrate 2-D or 3-D coarse-mesh engineering-scale simulation tools like PRONGHORN (for the core) and 1-D system analysis code SAM (for the primary loop and the plant) along with 3-D tools like Nek5000 (for the plena).

Table of Contents

LIST OF FIGURES

LIST OF TABLES

1 INTRODUCTION

For safety and licensing purposes, we must analyze the transient response of high-temperature gas cooled reactors (HTGR) to hypothetical accident scenarios including Pressure Conduction Cooldown (PCC) [1-2]. The PCC is often associated with a loss of offsite electrical power resulting in failure of the blower to force coolant into the core, the reactor is scrammed and structural integrity remains intact such that there is no loss of coolant mass. Decay heat is removed by natural circulation of the helium coolant, which requires that the flow be reversed from forced downward flow to buoyancy-driven upward flow. The resulting flow and temperature distribution is complex, as coolant rises from the lower plenum to up through the core and upper plenum, and between the reflector and the core (Figure 1-1(b)). There is a potential for the heat transfer to be degraded during the transition to natural circulation as coolant in the channels may shift from a turbulent to a laminar flow regime. Further, there is a concern that hot plumes arising from the core channels may impinge on the structures in the upper plenum, exposing components to locally high temperatures and significant thermal gradients.

Advanced computational tools can help evaluate the sensitivity of the behavior of these hot plumes to reactor design parameters like channel geometry, number of channels, and heating profiles. One of the first steps in developing such an advanced capability is to validate existing Computational Fluid Dynamics (CFD) tools for analysis of jet mixing and Deteriorated Turbulent Heat Transfer (DTHT) in geometries similar to the upper plenum and coolant channels, respectively. Such a simulation campaign is underway, using the CFD codes Nek5000 and STAR-CCM+, to analyze the $1/16^{th}$ scale Very High Temperature Reactor (VHTR) upper plenum and DTHT experiments performed at Texas A&M University (TAMU) and Massachusetts Institute Technology (MIT), respectively. In the TAMU VHTR experiments, fluid enters a lower plenum from a horizontal inlet pipe, splits into several vertical inlet channels, and enters the scaled dome-shaped test section, where the jet mixing occurs [5-7]. In the DTHT experiments, a simple vertical cylindrical tube was used for wall-heated flows similar to the coolant channels in HTGR [10-12].

In our previous work [5], CFD model investigations of jet velocities for various upper plenum configurations analyzed in both simplified and moderately complex geometries. Significant deviations were found in the predicted jet velocities when compared to experimental data, when considering only the upper plenum with simplified inlets and symmetric outlet. Also, the flow asymmetry was not predicted as in experiments due to the assumption of identical mass flow rates in each coolant channel (five coolant channel configuration). That work concludes that a full geometry model including both lower plenum and asymmetric outlet is necessary to predict the flow asymmetry in the upper plenum.

In this report, simulation results were analyzed for various Reynolds (Re) flows from 50 to 3413 in a single coolant channel configuration. Moreover, the axial jet velocities were verified in two different CFD codes, Nek5000 and STAR-CCM+, for laminar and turbulent Reynolds flows (200, 500 and 3413). In addition, the full geometry simulations were included for five coolant channels to validate with experimental data. Further, the CFD codes were verified and validated with DTHT benchmark test data. The details of the DTHT regimes in a PCC event were discussed in the following paragraph.

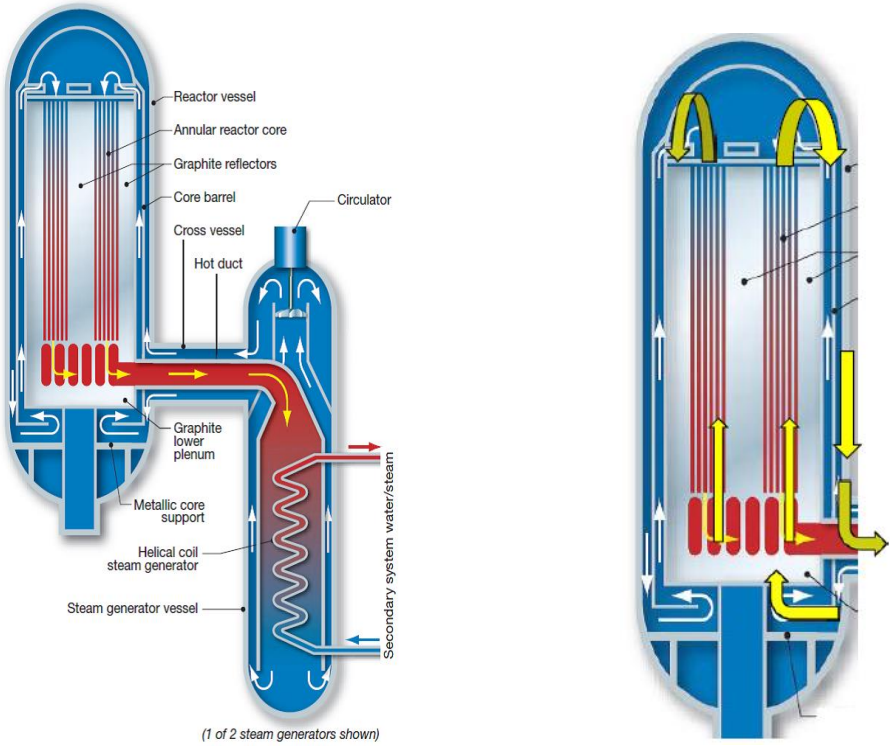

(a) (b)

Figure 1-1. HTGR (a) under normal operating conditions, (b) natural circulation (yellow arrows) pathways during Pressurized Conduction Cooldown

The DTHT conditions can be encountered in a nuclear system during an anticipated transient. In particular, the Generation IV gas-cooled reactor, which has generated a considerable interest and is under development in the U.S., France, and Japan, has a possibility to operate in the DTHT regime during post-loss-of-coolant accident (LOCA) conditions [8-9]. In Lee et al. [10-11], experiments were conducted to study the Deteriorated Turbulent Heat Transfer (DTHT) regime in gas up-flow. The DTHT regime is defined as the deterioration of normal turbulent heat transport due to acceleration and buoyancy effects. In their work, the detailed description of an experimental facility is provided. Both the acceleration driven DTHT and the buoyancy driven DTHT showed a reduction of heat transfer coefficient of up to 70% compared to the normal turbulent heat transfer.

In this report, 3D CFD models were verified and validated with two different benchmark tests; (i) the TAMU 1/16th scale VHTR and (ii) MIT's DTHT benchmark test.

2 MODELING AND SIMULATIONS OF 1/16TH SCALE VHTR UPPER PLENUM

2.1 TAMU VHTR Benchmark Test

As seen in Figure 2-1, the 1/16th scale VHTR experimental design consists of a lower plenum, an upper plenum, core channels, horizontal inlet and outlet pipes, and a water reservoir [6]. To validate CFD models, experimental data is only available for the five coolant channel configuration. Experiments are underway for the single coolant channel configuration at TAMU. The details of both single and multiple (five) coolant channel configurations are discussed in the following sub sections.

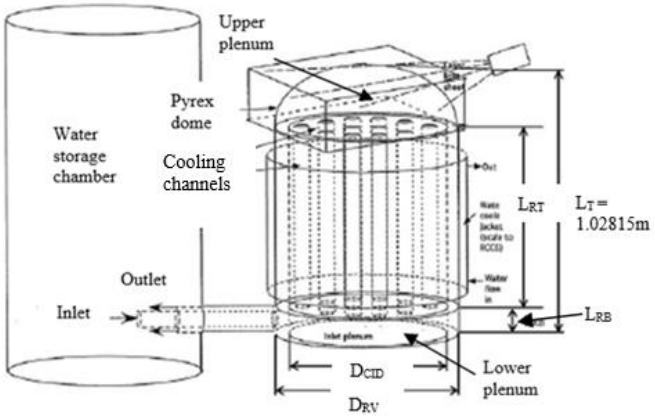

Figure 2-1. Texas A&M University 1/16th scale VHTR experiment [6]

2.1.1 Single Coolant Channel Configuration

As shown in Figure 2-2, the jet flow is allowed in a single coolant channel and the remaining 24 channels were closed. The opened channel is at the center of all of the coolant channels and is highlighted in Figure 2-2. In this configuration, both inlet and outlet channels were simplified due to the negligible influence on jet velocities in the upper plenum. In contrast, full geometry simulations are required for multiple jets due to non-identical mass flow rates in each coolant channel as discussed in the following Section (Section 2.1.2).

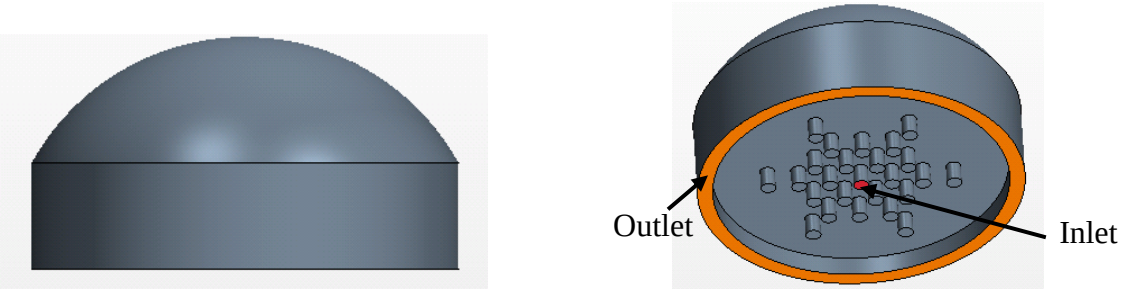

(a) (b)

Figure 2-2. Simplified model geometry for single coolant channel flow, (a) side view, and (b) visible view of inlet and outlet.

3D CFD isothermal Large Eddy Simulations (LES) were performed using Nek5000. The single-jet CFD model results from Nek5000 were also verified with the STAR-CCM+ Reynolds Stress Model (RSM). In these models, a fully developed inlet flow assumption was considered due to sufficient coolant channel entrance length [5-7]. The geometry and operating conditions are shown in Table 2-1 and Table 2-2 [6-7].

Table 2-1. TAMU 1/16th scale VHTR dimensions

Plenum diameter, D_{RV} [m]	0.4083
Inner core diameter, D_{CID} [m]	0.37
Upper plenum height [m]	0.197
Coolant channel diameter [m]	0.01905
Number of coolant channels	25
Coolant channel height, L_{RT} [m]	0.7749
Lower plenum depth, L_{RB} [m]	0.05625
Lower plenum diameter, D_{CID} [m]	0.37

Table 2-2. Operating conditions and thermo physical properties for single coolant channel configuration

Reynolds number (Re)	50 to 3413
Inlet temperature [K]	292 -317
Outlet pressure [Pa]	0.0
Water viscosity [Pa.s]	9.83E-4 – 6.06E-4

2.1.2 Five Coolant Channel Configuration

As shown in Figure 2-3, the jet flow is allowed in five coolant channels and the remaining 21 channels were closed. The opened channels are highlighted in Figure 2-3(b). In this multi-jet configuration, a parallel horizontal inlet and outlet were considered similar to the experimental geometry. Fluid enters in a lower plenum and subsequently the mass flow splits into each coolant channel. The mass flow rates in each coolant channel are not identical due to the horizontal inlet (Figure 2-3(a)).

3D CFD isothermal simulations were performed using STAR-CCM+ for the TAMU multi-jet model. The geometry and operating conditions are shown in Table 2-1 and Table 2-3 [6-7].

Table 2-3. Operating conditions and thermo physical properties for five coolant channel configuration

Approx. Reynolds number in each channel	422
Total mass flow rate [kg/s]	0.018689
Inlet temperature [K]	317
Outlet pressure [Pa]	0.0
Water viscosity [Pa.s]	6.06E-4

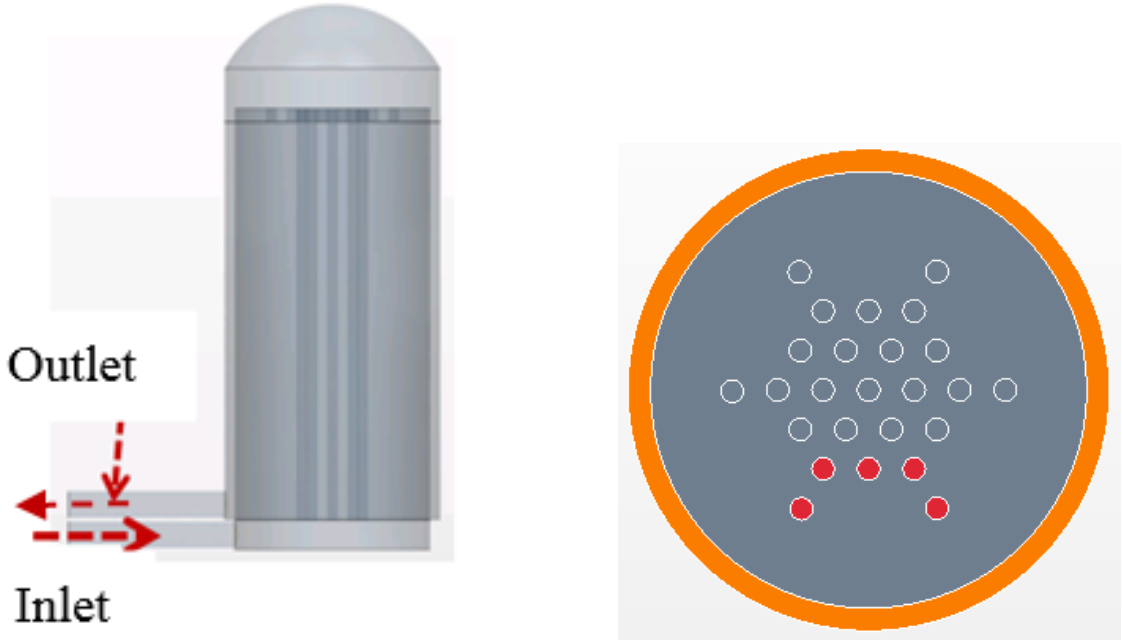

(a) (b)

Figure 2-3. Modeled geometry for five coolant channel flow, (a) side view, and (b) upper plenum bottom view.

2.2 Numerical Modeling

3D CFD modeling and simulations were performed using STAR-CCM+ and Nek5000. The STAR-CCM+ code uses the Finite Volume (FV) method and the Nek5000 uses the Spectral Element Method (SEM) to solve the Navier-Stokes fluid flow equations, numerically. The merit of Nek5000 is that it is a highly scalable, open source, transient CFD code and it has run on over one million processors on Argonne's massively parallel Blue Gene/Q computer, Mira [3].

In STAR-CCM+, the velocity and Reynolds stress turbulence equations were solved using an incompressible, steady state, isothermal, segregated flow solver [4]. In Nek5000, the velocity equations were solved using an incompressible, transient, isothermal, Helmholtz solver [3]. The model description for both Nek5000 and STAR-CCM+ are shown in Table 2.4.

In this work, simulations were performed until the specified flow convergence criteria were met. The residuals were set to drop around five orders of magnitude in STAR-CCM+ and Nek5000 models.

In Figure 2-4 and Figure 2-5, two different meshes were considered for numerical simulations: (1) polyhedral mesh in STAR-CCM+ and (2) Hexahedral mesh in Nek5000. The simulation results were shown at measured plane where the experimental PIV data is available. In both Nek5000 and STAR-CCM+, a very fine mesh (~0.3mm) was selected around the inlet jet where the maximum velocity gradients can exists.

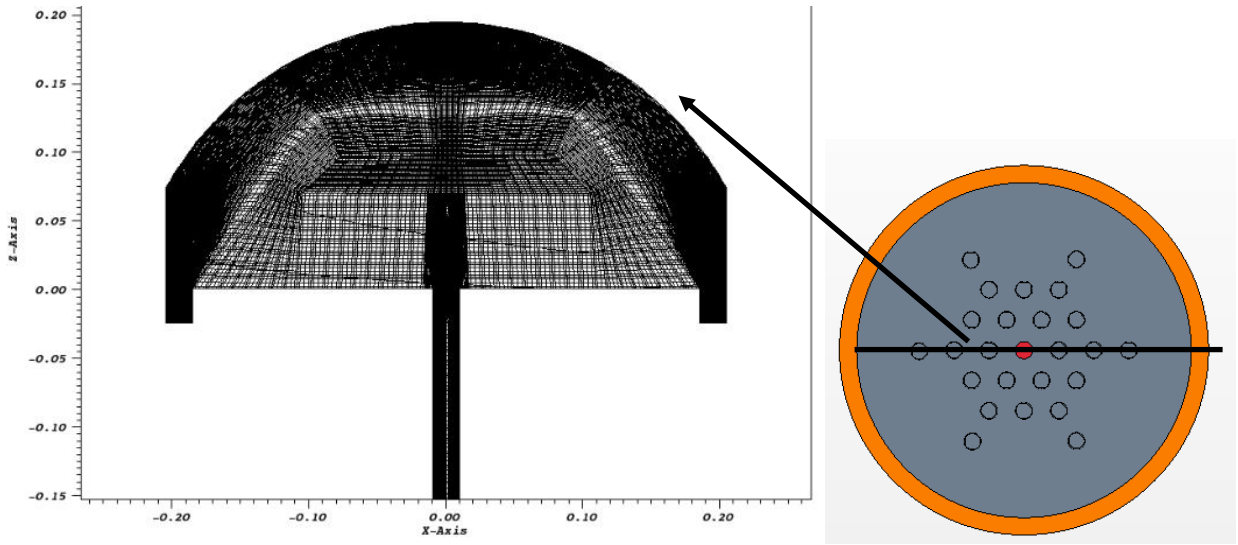

(a) (b)

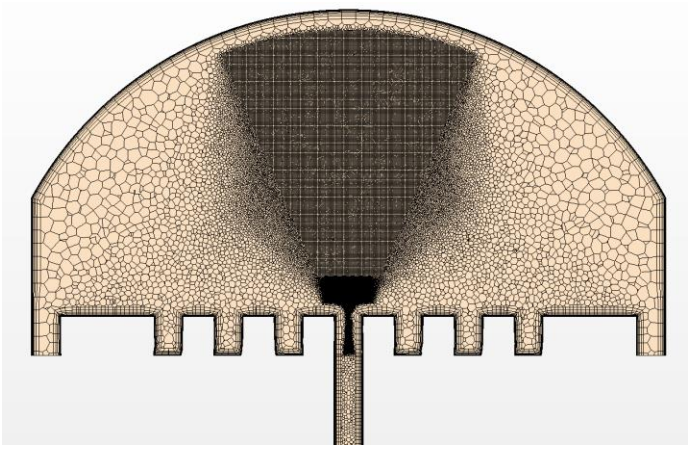

(c)

Figure 2-4. Upper plena mesh for a single coolant channel on a vertical plane at center of the coolant channel; (a) Nek5000 hexahedral mesh, (b) Top view and (c) STAR-CCM+ polyhedral mesh.

Table 2-4. CFD model description for 1/16th scale VHTR

	STAR-CCM+- v12.02	Nek5000
3D Simulations	Isothermal Steady State	Isothermal Transient
Numerical Method	Finite Volume	Spectral Element
Turbulence	RSM, laminar	Large Eddy Simulations (LES)
Liquid Phase	Water	Water
Mesh No. of Elements/points [Millions]	1.8 - 50	31 – 102 [Gauss–Legendre–Lobatto (GLL) points]

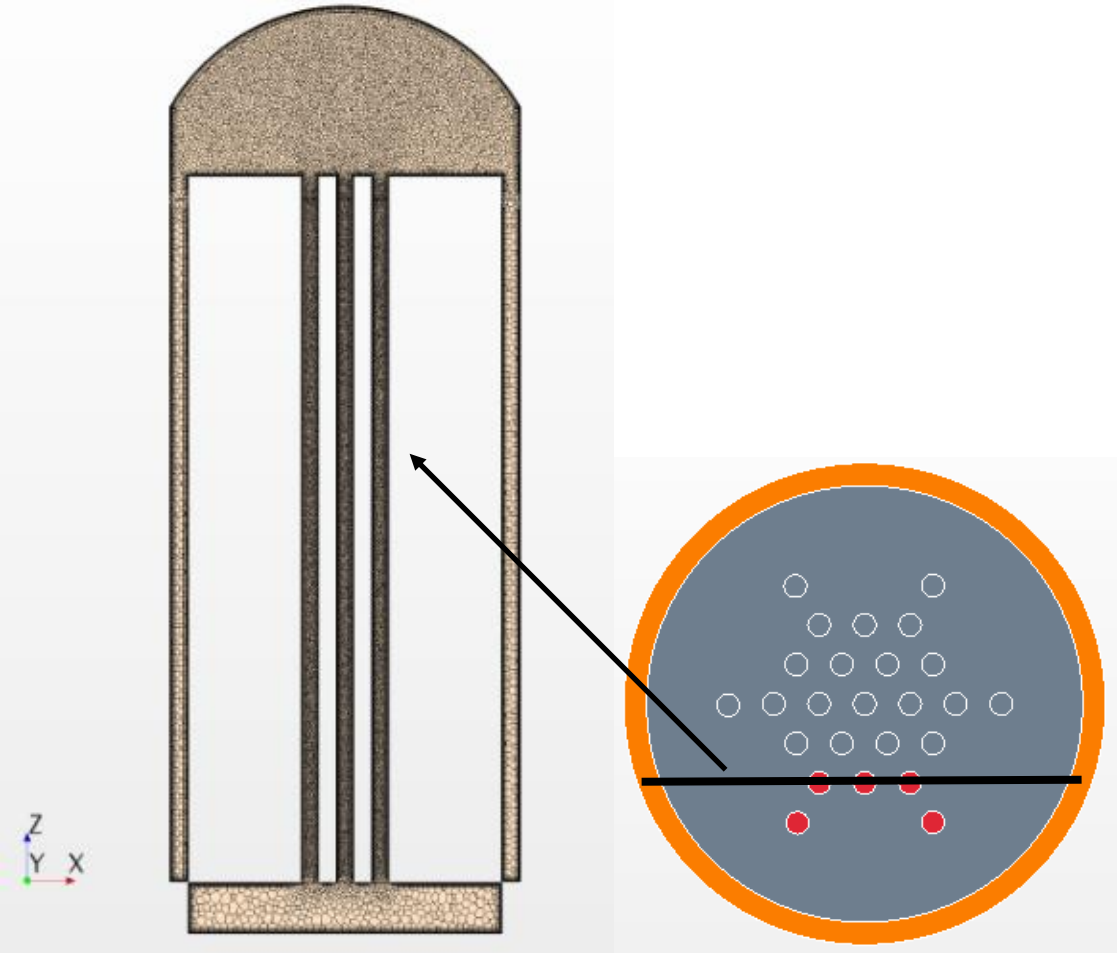

(a) (b)

Figure 2-5. STAR-CCM+ polyhedral mesh for five coolant channels with a lower plenum and a horizontal inlet and outlets; (a) measured vertical plane, and (b) top view

The volume mesh was generated to simulate the configurations shown in Figure 2-5. The minimum volume cell edge size was set at 1 mm over the solid surface and the maximum cell edge size was allowed up to 4 mm away from the solid surface. A total of six prism layers were selected over the surfaces with a total thickness of 6mm.

2.3 Grid Independence Study

In the following section, the presented results were grid independent from both CFD tools (Nek5000 and STAR-CCM+). Two different meshes were studied to justify grid independence of jet axial velocities for the single coolant channel configuration (Re of 500). As seen in Figure 2-6, the predicted axial velocities along the center of the jet were consistent in both fine and coarse meshes. In Nek5000, simulations were performed on a hexahedral mesh whereas in STAR-CCM+ simulations were performed on polyhedral mesh.

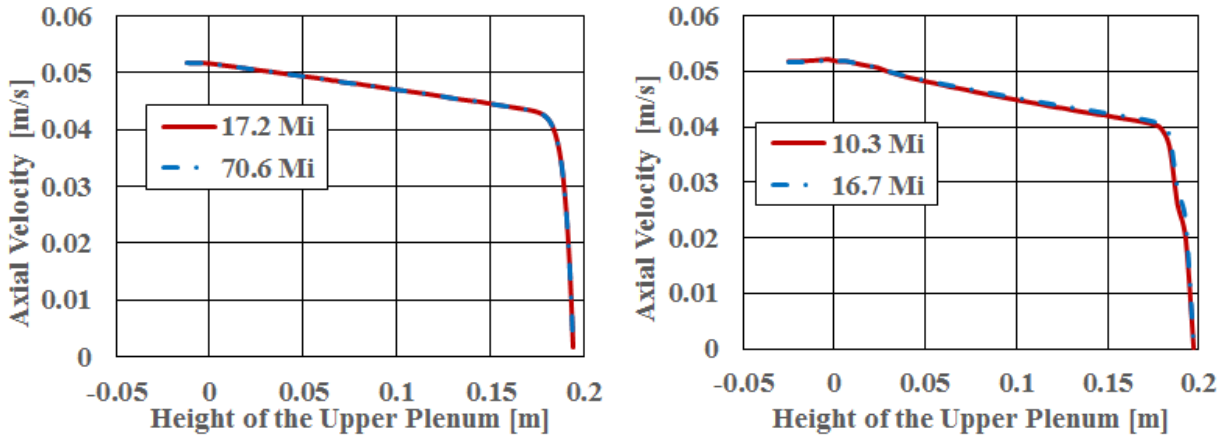

(a) (b)

Figure 2-6. Comparison of axial velocities along the center of the single jet (Figure 2-2(b)) for different mesh count for Re of 500; (a) Nek5000 and (b) STAR-CCM+.

2.4 Results and Discussion

In this section, STAR-CCM+ and Nek5000 simulation results were analyzed for a single coolant channel. On the other hand, only the STAR-CCM+ analysis for the five coolant channels was included in this report, which will be analyzed by Nek5000 in the future.

2.4.1 Single Coolant Channel

As seen in Figure 2-2, a single channel is considered at the center of the core or upper plenum. In this section, Nek5000 simulations were performed and analyzed for various Reynolds flows from 50 to 3413. Furthermore, the axial jet velocities were analyzed by two different CFD tools (Nek5000 and STAR-CCM+).

As seen in Figure 2-7(a-c), stagnant flow zones were observed near the upper plenum hemisphere due to low velocities (Re=200,100 and 50). Significant flow mixing was observed for higher Reynolds flows (Re>500) (Figure 2-7(d-e)). For Re < 200, the jet penetration length and spread rate increases with an increase of Reynolds number. For Re>500, the jet reaches the upper plenum hemisphere where jet impingement may lead to hot spots on the wall surface in non-isothermal flows. In high Reynolds number flows (Re >500), multiple recirculation zones were observed in the off side of the jet. In the VHTR, these recirculation zones are undesirable where hot or cold fluids can be trapped leading to high thermal gradients in non-isothermal flows.

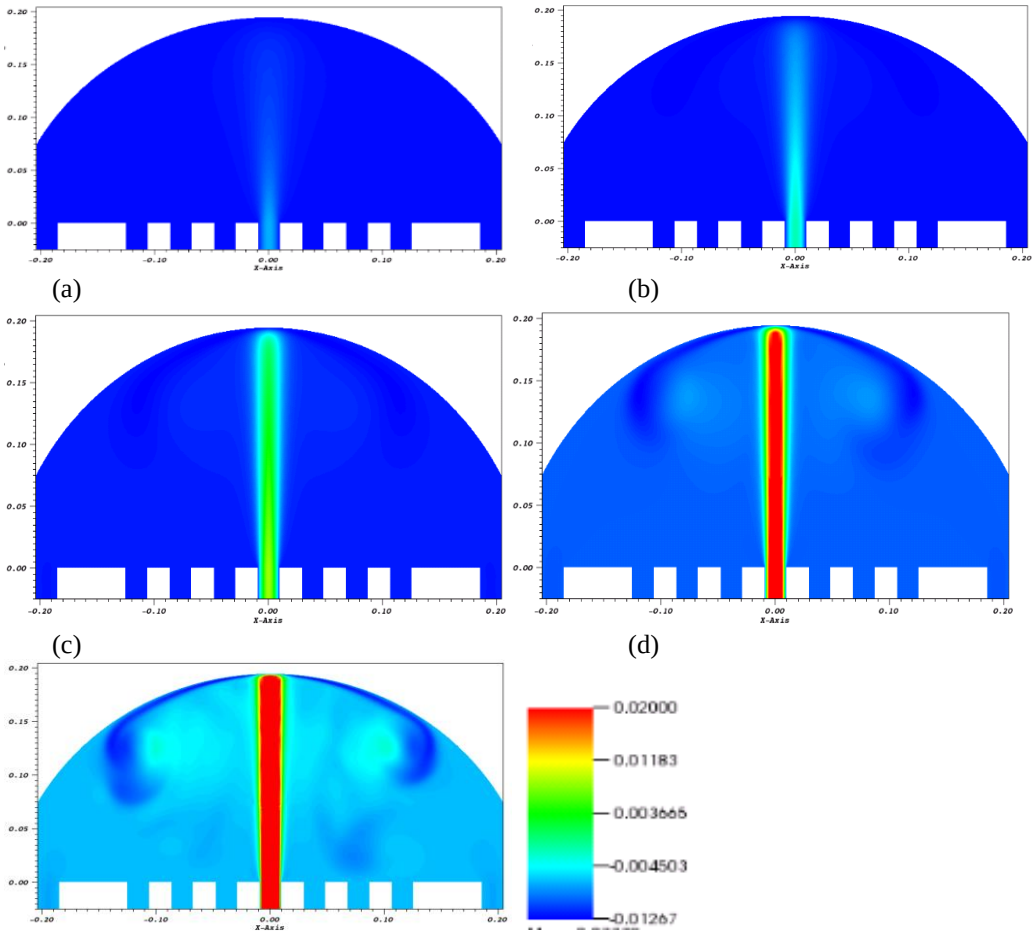

Figure 2-7. Comparison of axial velocities over measured plane in Nek5000; (a) Re=50, (b) Re=100, (c) Re=200, (d) Re=500, and (e) Re=1000. Fluid properties considered at temperature of 317 K.

As seen in Figure 2-8, axial velocity at the center of the jet diminishes close to the upper plenum hemisphere (0.195 m). The spread rate of the stagnation zone increases with decrease of Reynolds number. In non-isothermal low Reynolds number flows, the momentum or jet behavior in the upper plenum can be overtaken by the plume due to significant density changes. Future work includes the study of non-isothermal flows to characterize the jet and plumes in the VHTR. Furthermore, the Nek5000 simulation results will be validated with the experimental data**,** which are currently underway at TAMU for ASME V&V 30 benchmark test.

As seen in Figure 2-9, the observed axial jet velocities were comparable in both CFD tools (Nek5000 and STAR-CCM+) for Re of 200, 500 and 3413. At high Re (>500), the deviations may be due to different turbulence models, i.e. RSM in STAR-CCM+ and LES in Nek5000. Nonetheless, an experimental validation is required to comment on the superiority of these codes. In Figure 2-9 and Figure 2-10, the time averaged (20 sec) axial velocities were presented for Nek5000 to verify with STAR-CCM+ RSM results.

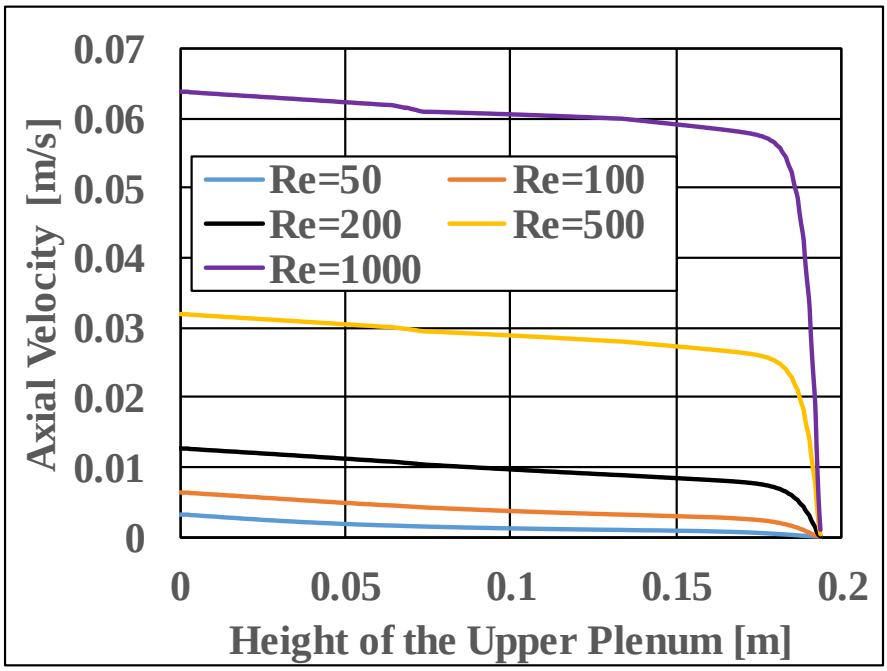

Figure 2-8. Comparison of axial velocities along the center of the jet. Fluid Properties considered at temperature of 317 K.

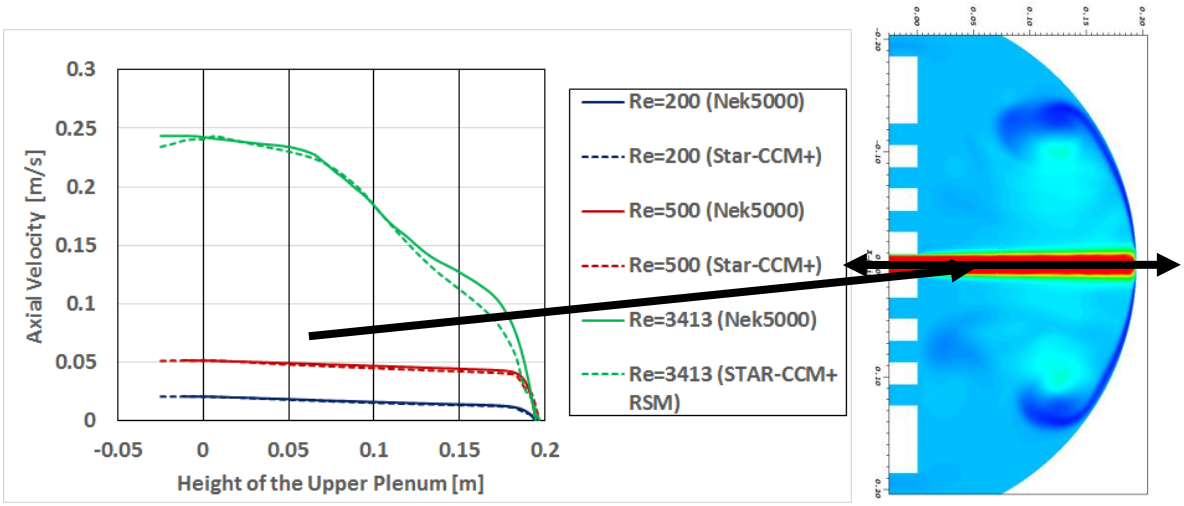

Figure 2-9. Comparison of axial velocities along the center of the jet using Nek5000 and STAR-CCM+. Fluid properties considered at temperature of 291.74 K.

Near the upper plenum inlet, the axial velocity profiles were compared in both codes, i.e, Nek5000 and STAR-CCM+, across the radius and the axis as shown in Figure 2-9 and Figure 2-10. Towards an upper plenum hemisphere (13cm to 019cm), the found deviations may be due to the inherent differences of the turbulence models, as discussed above. Near the upper plenum inlet, the calculated jet velocities using both CFD tools, STAR-CCM+ RSM and NEK5000 LES, were comparable with a marginal deviation. Near the upper plenum hemisphere, the predicted jet velocities are uniform with the STAR-CCM+ than the Nek5000 turbulence models (Figure 2-10). This may be due to higher turbulence in RSM compared to LES.

As seen in Figure 2-11, turbulence behavior was demonstrated in the axial velocity instantaneous fields for Reynolds number of 3413 using Nek5000 transient simulations.

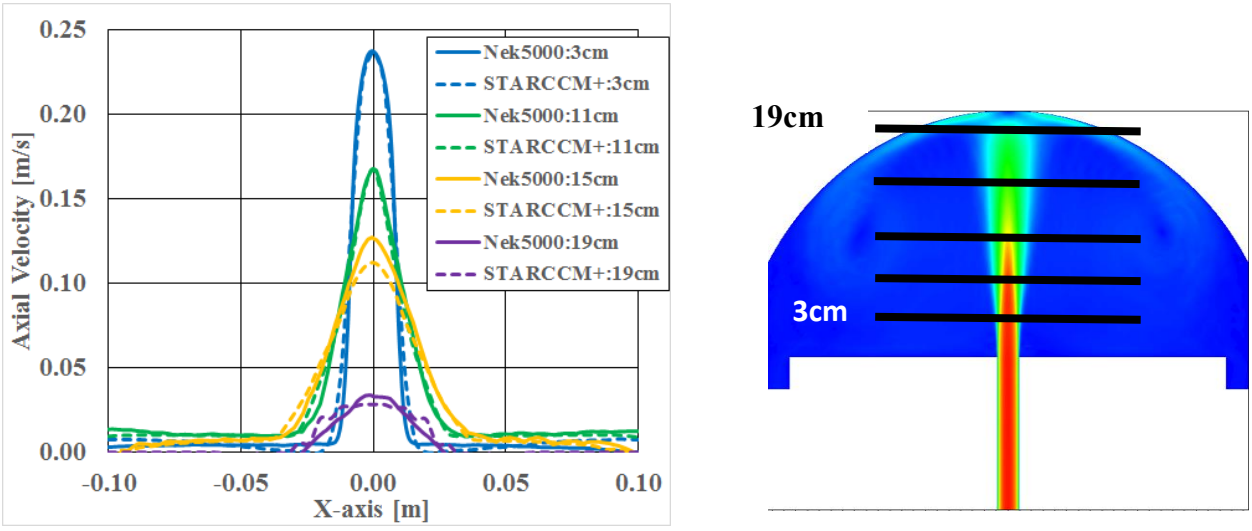

Figure 2-10. Comparison of time averaged (20 sec) axial velocities across radial direction at various axial locations (y=0). Fluid properties considered at temperature of 291.74 K.

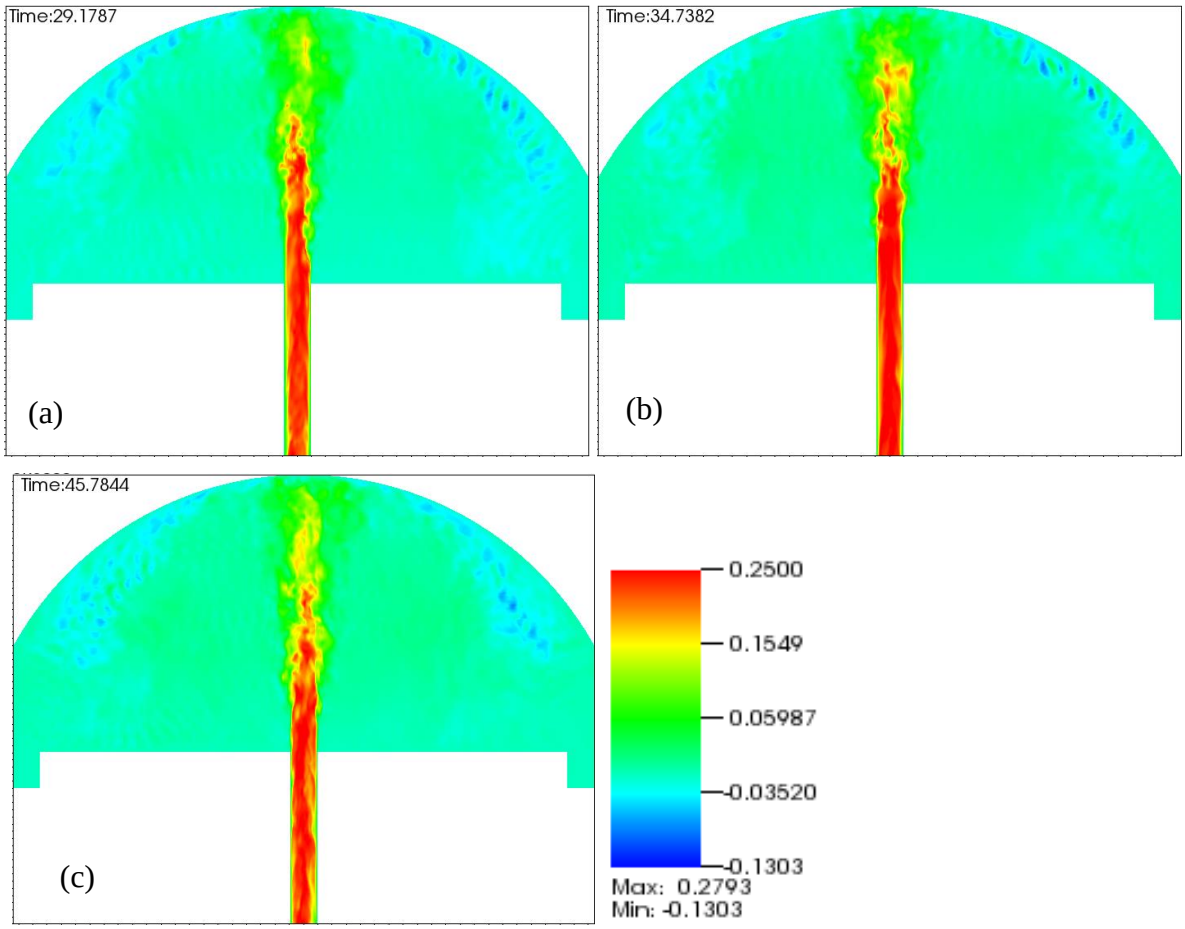

Figure 2-11. Nek5000 instantaneous axial velocities at various physical times for Re of 3413; (a) 29.17 sec, (b) 34.73 sec and (c) 45.78 sec. Fluid properties considered at temperature of 291.74 K.

2.4.2 Five Coolant Channels

In this section, STAR-CCM+ simulation results of the five coolant channel configuration (Figure 2-3(b)) were analyzed and compared with the available measured data from Kyle et al. [13]. To be noted, the Nek5000 simulations were not included due to limited available time to prepare the mesh for the full geometry apart from the heavy computational time.

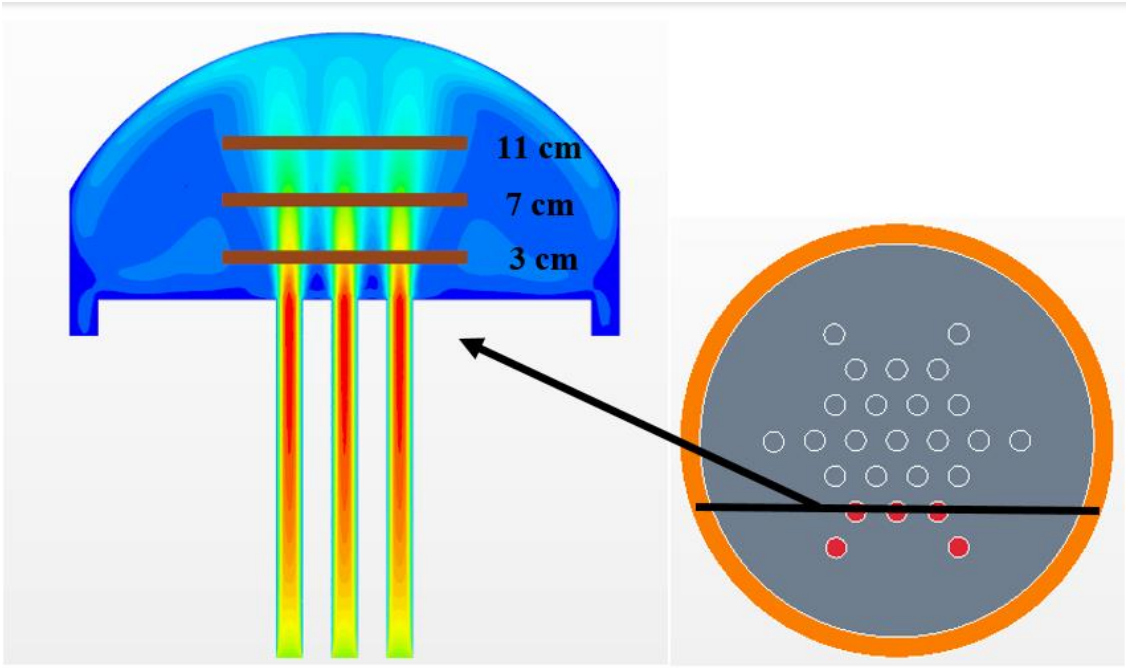

(a)

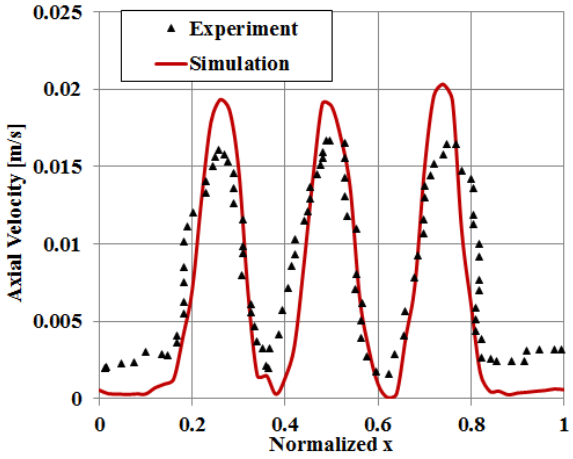

(b)

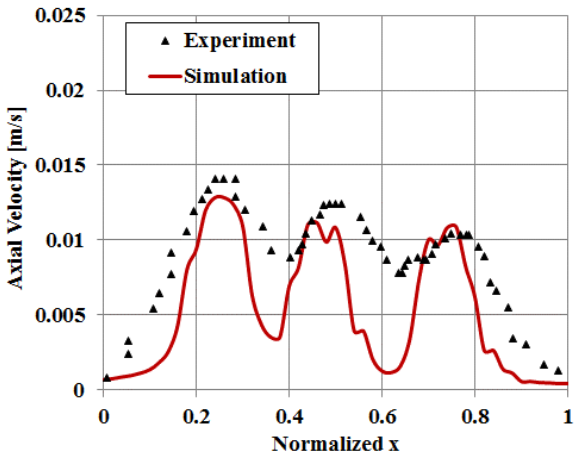

(c)

Figure 2-12. Comparison of axial velocities for Re of 422: (a) Contour plot of STAR-CCM+ predictions in measurement plane over three side-by-side coolant channels in a five coolant channel geometry (b) comparison of measurements to code axial velocity predictions at 3 cm and (c) 11 cm, from inlet of the upper plenum. Fluid properties considered at temperature of 317 K.

From Figure 2-12, the STAR-CCM+ model axial velocity predictions were qualitatively agreed with the experimental data. Also, an asymmetric flow pattern was observed similar to experiments at measurement location of 11cm (Figure 2-12(c)). Furthermore, the calculated peak velocities were comparable with the experiments at 11cm (near the upper plenum hemisphere). Near the upper plenum inlet (3cm), the simulated peak velocities were overpredicted when compared to the experimental data. In contrast, the simulated off side peak velocities were underpredicted in both measured locations (3cm and 11cm). This indicates that the numerical simulations were less diffusive than the experiments. In simulations, the found deviations may be due to the assumption of a constant velocity at the inlet instead of using real time measured velocities as in experiments (fluctuates around ±3% averaged velocity). In general, the velocity fluctuations enhance the mixing rates in the upper plenum. Further investigation may be required to study the inlet effects on velocity profiles.

2.5 Conclusions

3D CFD simulations were performed to analyze the available experimental data for the upper plenum of the Texas A&M University 1/16th scale VHTR. In the five coolant channel configuration, an asymmetric flow pattern was observed similar to the experiments using STAR-CCM+. The observed jet peak velocities were in good agreement with the experimental data. The found deviations in the off side of the jet may be due to the assumption of constant velocity at the inlet, instead of using velocity fluctuations as in the experiments (±3% averaged velocity). Further investigation may be required to study the inlet effects on velocity profiles.

In the single coolant channel configuration, stagnation zones were observed near the upper plenum hemisphere for Re<500. Significant fluid mixing was observed for high Reynolds flows (Re>500). The observed jet velocities were identical in both CFD tools (STAR-CCM+ and Nek5000), with a marginal deviation in the single coolant channel.

3 MODELING AND SIMULATIONS OF DETERIORATED TURBULENT HEAT TRANSFER IN WALL HEATED CYLINDRICAL TUBE

3.1 DTHT Benchmark Test

The DTHT can be encountered in a nuclear system during an anticipated transient. In particular, the Generation IV gas-cooled reactor, which has generated a considerable interest and is under development in the U.S., France, and Japan, has a possibility to operate in the DTHT regime during post-loss-of-coolant accident (LOCA) conditions [8-9]. In Lee et al. [10-11], experiments were conducted to study the Deteriorated Turbulent Heat Transfer (DTHT) regime in gas up-flow (Figure 3-1). The DTHT regime is defined as the deterioration of normal turbulent heat transport due to acceleration and buoyancy effects. In their paper, the detailed description of the experimental facility is provided. Both the acceleration driven DTHT and the buoyancy driven DTHT showed a reduction of heat transfer coefficient up to 70% compared to the normal turbulent heat transfer.

3.2 Geometry and Operating Conditions

As seen in Figure 3-1, the experiment loop connecting ~2m-long heated section with elevated cooler and has an overall height of 7m spreading over 2 floors to maximize a natural circulation capability. The first system is the main loop, where most of the measurements are made. The main loop further divided into three sections - test section, chimney section and downcomer section. The loop is designed to operate at pressures of 1MPa and wall temperature of 1000K [8-12]. The objective of this work is to verify and validate CFD tools with the test section measured data. As seen in Figure 3-2, simulations were performed only for the test section with an extended inlet and outlet to generate a fully developed flow and to minimize the outlet effects on the test section, respectively. For DTHT benchmark test, the modeling and simulations were performed for a given operating conditions as shown in Table 3-1. In Nek5000, recycling boundary condition was applied to generate a fully developed flow in a short extended inlet section (Figure 3-2(b)). In contrast, a full-length extended inlet (Figure 3-2(a)) simulations were performed for STAR-CCM+.

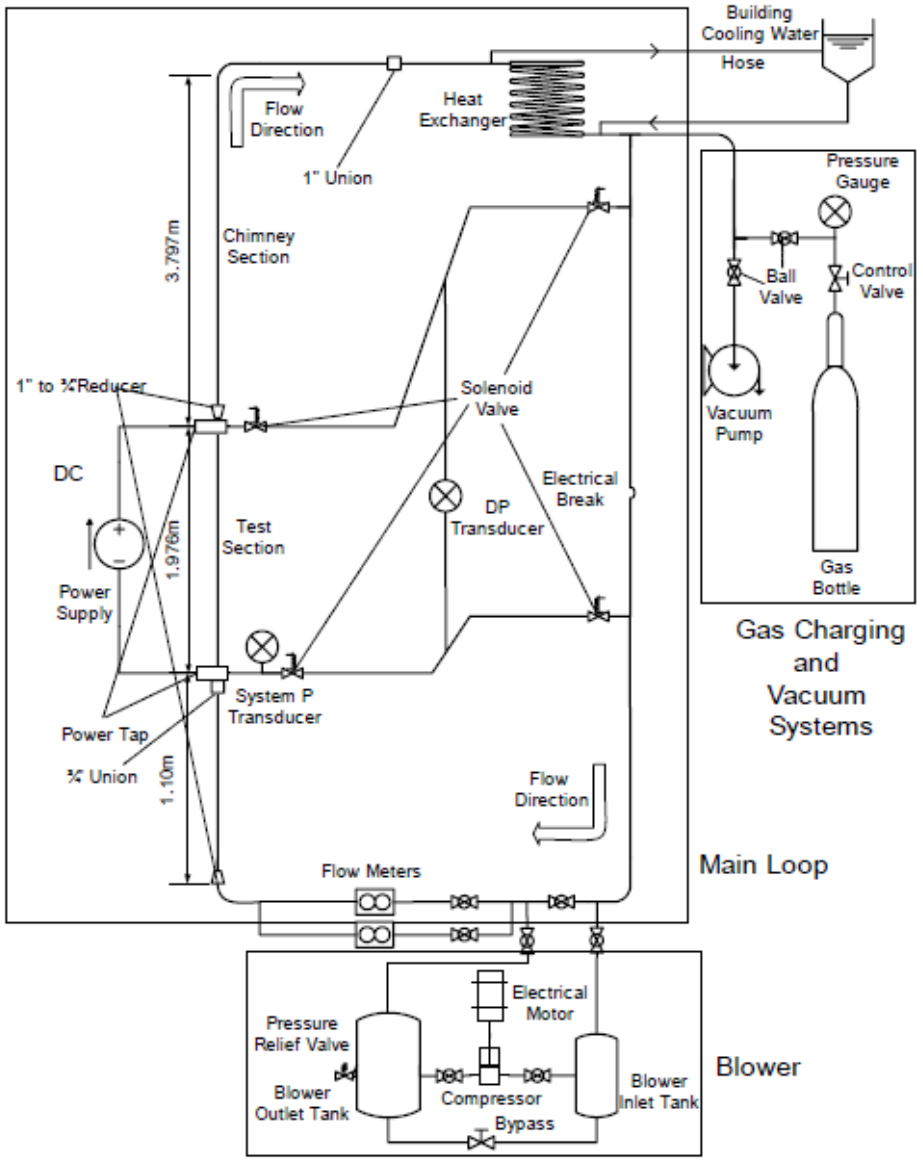

Figure 3-1. Schematic diagram of DTHT benchmark test [10]

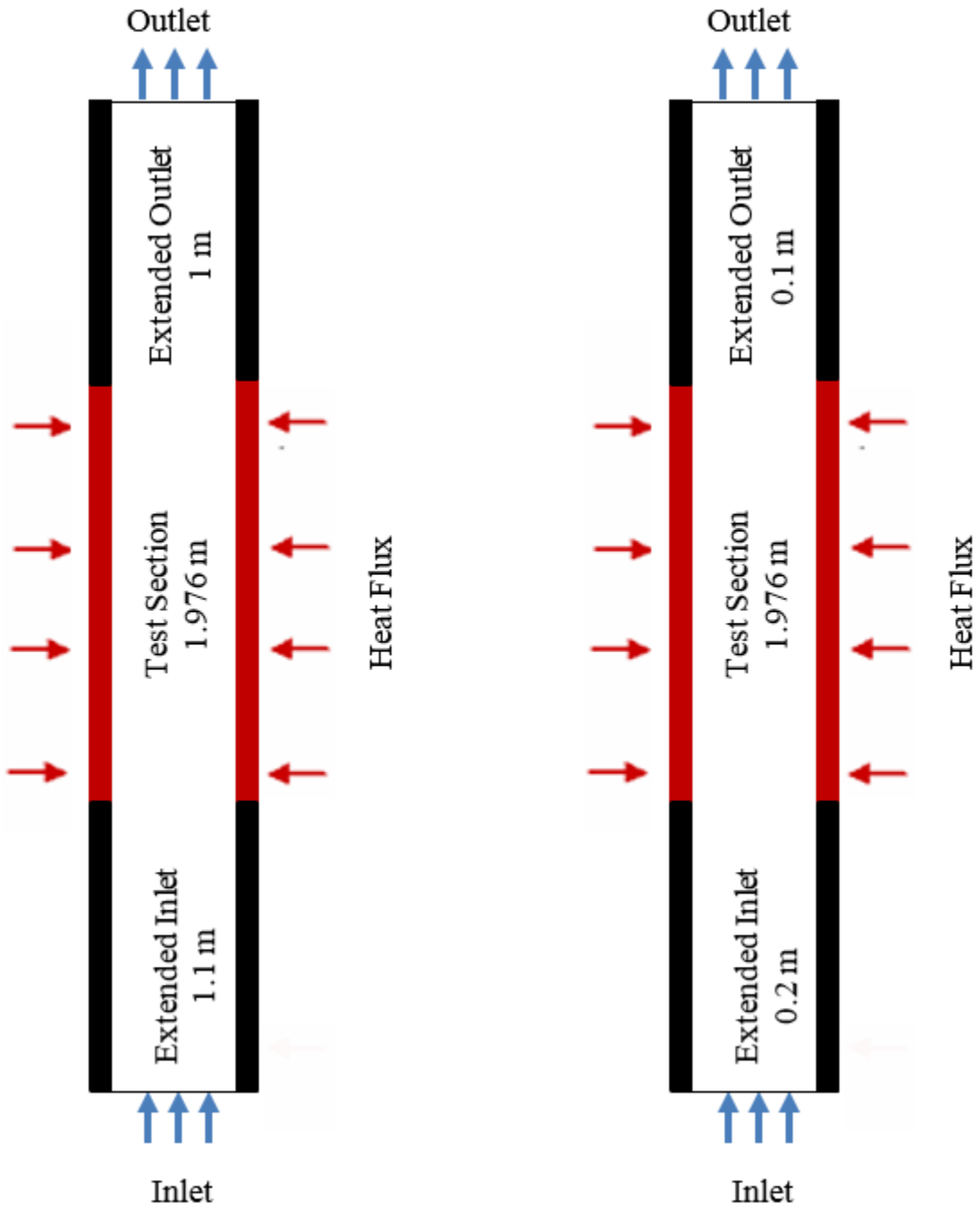

Figure 3-2. Modeled geometry for DTHT benchmark test; (a) STAR-CCM+ and (b) Nek5000

Table 3-1. DTHT benchmark test operating conditions for inlet temperature of 304 K [11]

RUN	Reynolds Number (Re)	Wall heat [W/m^2]
4	8927	9356
5	6716	5572
6	6667	4675

3.3 Numerical Modeling

3D CFD modeling and simulations were performed using STAR-CCM+ and Nek5000. The STAR-CCM+ code uses the FV method and the Nek5000 uses the SEM to solve the Navier-Stokes fluid flow equations, numerically (Table 3-2). In STAR-CCM+, the velocity and Reynolds stress turbulence equations were solved using compressible, steady state, real gas, non-isothermal, segregated flow solver [4]. In Nek5000, the velocity equations were solved using low Mach approximation, transient, real gas, non-isothermal, Helmholtz solver [3]. In this work, simulations were performed until the specified flow convergence criteria were met. The residuals were set to drop around five orders of magnitude in STAR-CCM+ and five orders of magnitude in Nek5000 models.

In STAR-CCM+, polyhedral mesh was generated to simulate the configurations shown in Figure 3-3(a). The minimum cell edge size was set at 0.65 mm over the solid surface and the maximum cell edge size was allowed up to 2.5 mm away from the solid surface. Six prism layers were selected over the surfaces with a total thickness of 2mm. In contrast, hexahedral mesh was generated for Nek5000 simulations as shown in Figure 3-3(b). In Nek5000, the full 3D pipe volume was discretized with 13,650,000 Gauss–Legendre–Lobatto (GLL) points, using 3500 slices in the axial direction and 3900 points in each radial cross section with a minimum GLL point size of 0.6mm and 0.22mm, respectively.

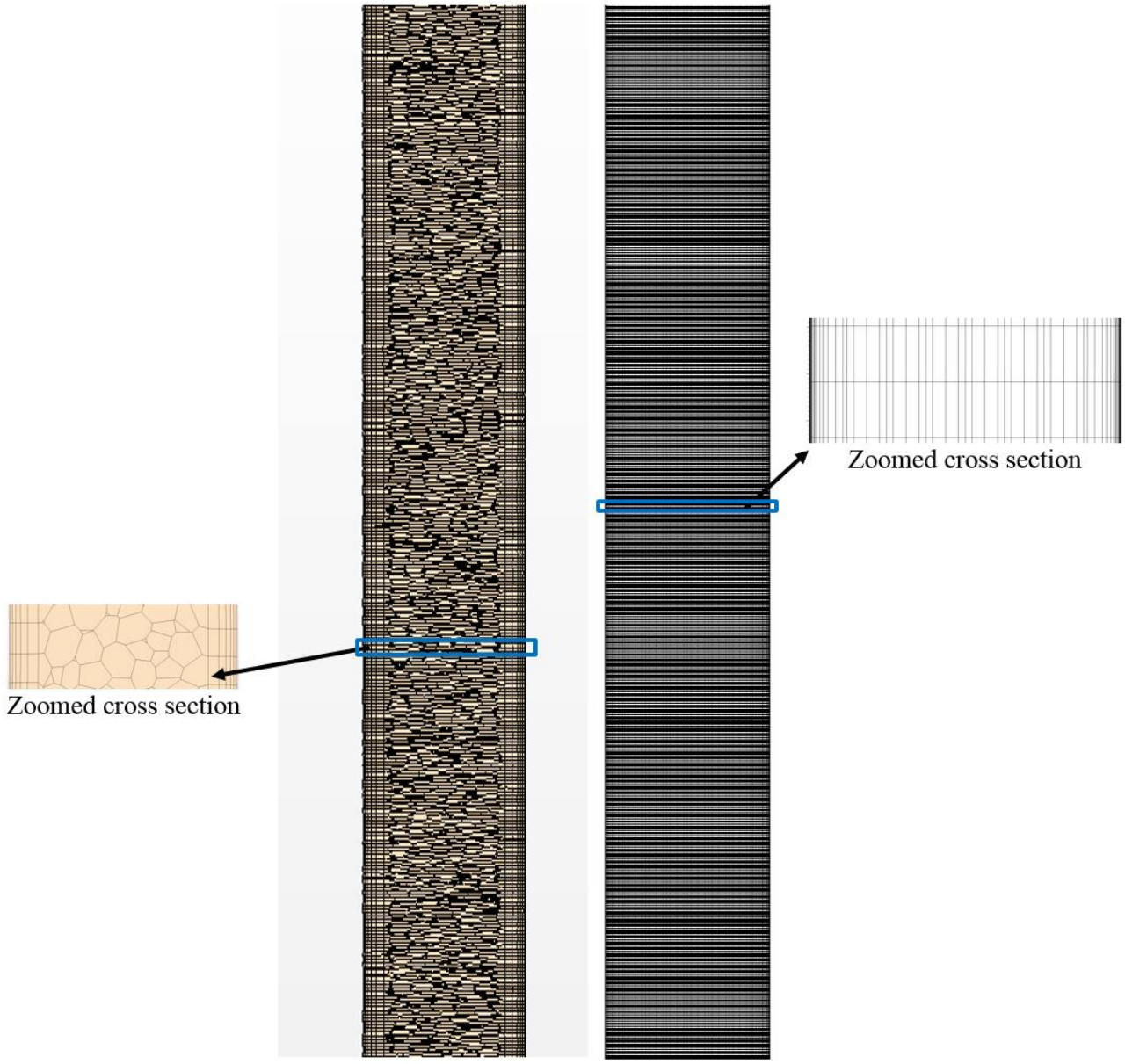

Figure 3-3. DTHT cylindrical tube mesh on a vertical plane at center of the tube; (a) STAR-CCM+ polyhedral mesh and (b) Nek5000 hexahedral mesh

Table 3-2. CFD model description for DTHT

	STAR-CCM+- v12.02	Nek5000
3D Simulations	Non-isothermal Steady State	Non-isothermal Transient
Numerical Method	Finite Volume	Spectral Element
Turbulence	RSM	Large Eddy Simulations (LES)
Gas Phase	Nitrogen	Nitrogen
Gas model	Real gas (NIST table)	Real gas (NIST table)
Mesh No. of Elements/points [Millions]	0.64	13.6 (GLL points)

3.4 Grid Independence Study

As in Figure 3-4, the DTHT results were verified with two different grids for STAR-CCM+ RSM. The negligible deviations were observed between both coarse and fine grids. Grid independence study concludes that the coarse grid is good enough to validate the CFD models for Run-6. Hence, the simulations were performed on the coarse grid for all runs as shown in Table 3-1. In STAR-CCM+, simulations were performed on a polyhedral mesh whereas in Nek5000 simulations were performed on a hexahedral mesh, as discussed above.

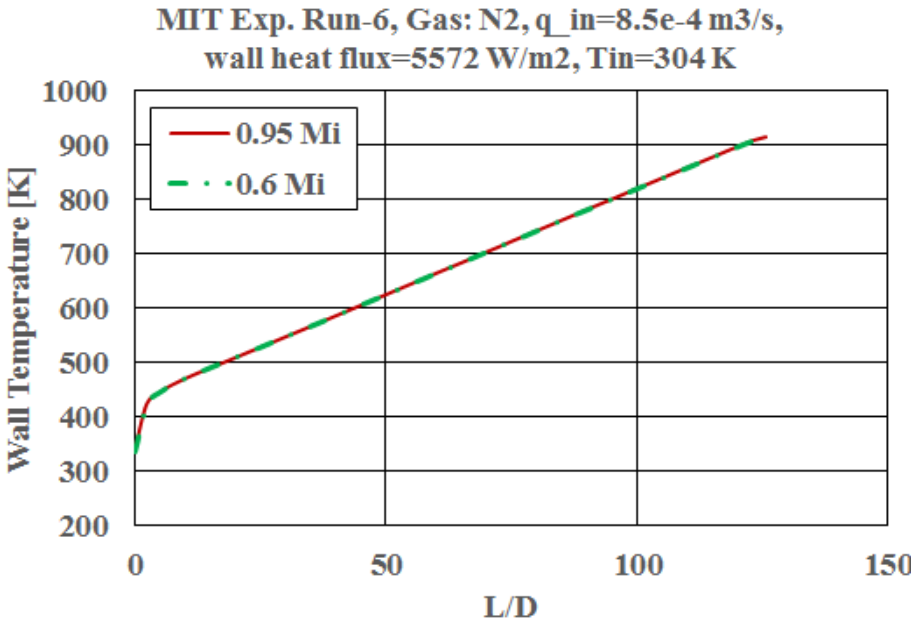

(a)

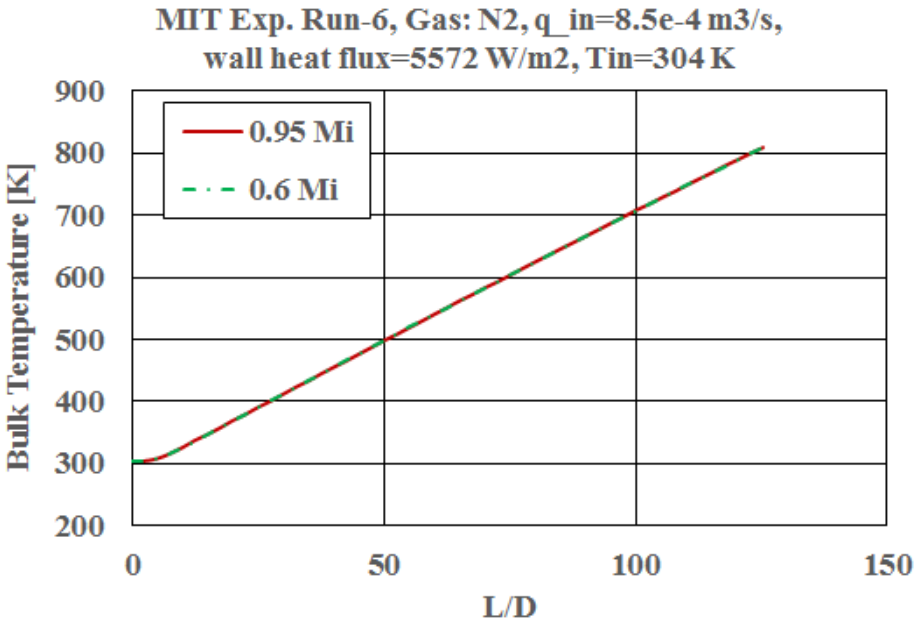

(b)

Figure 3-4. Comparison of temperatures along the tube (Figure 3-2) for different mesh count for Run-6 using STAR-CCM+; (a) Wall temperature and (b) Bulk temperature

3.5 Results and Discussion

In this section, three different DTHT experiments were modeled and simulated for a given operating conditions as shown in Table 3-1. These runs are named as Run-4, Run-6 and Run-7. For Run-6, both Nek5000 (LES) and STAR-CCM+ (RSM) CFD models were verified and validated with wall temperature data. For Run-4 and Run-7, only STAR-CCM+ RSM simulations were performed due to fast turnaround time compared to Nek5000 LES simulations.

In Figure 3-5, the calculated bulk temperatures were identical in both CFD codes, as expected. Good agreement was observed between both measured and calculated wall temperatures using Nek5000 simulations, except near inlet region. Near the inlet, the overpredicted wall temperatures may be due to lower turbulence predictions than the experiments. On the other hand, the underpredicted wall temperatures were observed using STAR-CCM+ RSM. This may be due to overpredicted turbulence with the STAR-CCM+ RSM. For Nek5000, the fluid temperature and velocity fields along the vertical plane (XZ) shown in Figure 3-6. The significant velocity rise was observed due to density drop in a wall-heated tube, towards an outlet. Near the wall region, the fluid temperature rise was observed due to constant wall-heat flux boundary condition. In the test section outlet, the sudden drop in measured wall temperatures were mainly due to axial heat loss by conduction to the power taps located at end of the heated section [11].

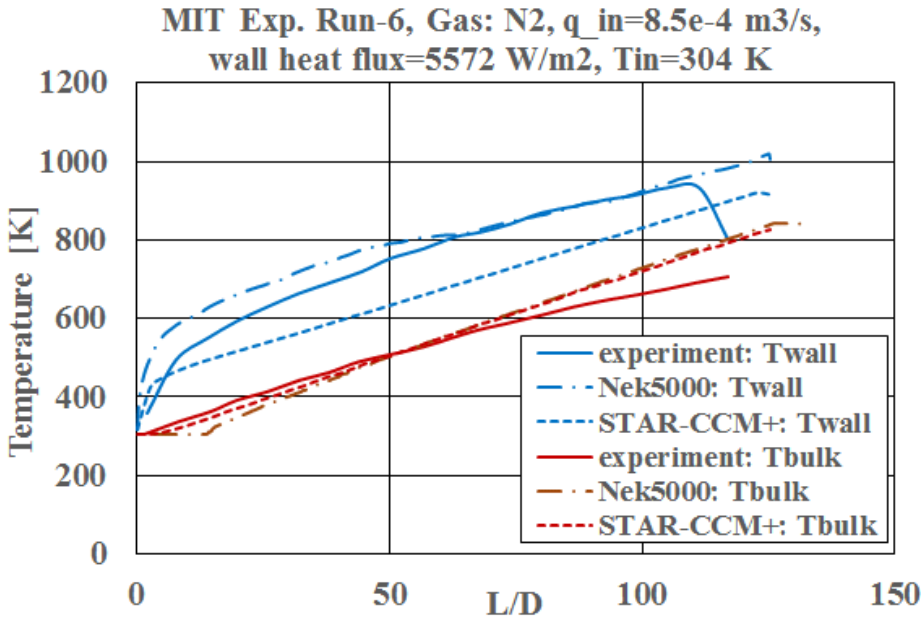

Figure 3-5. Comparison of wall and bulk temperatures along the axial direction of the test section using Nek5000 and STAR-CCM+ RSM for Run-6.

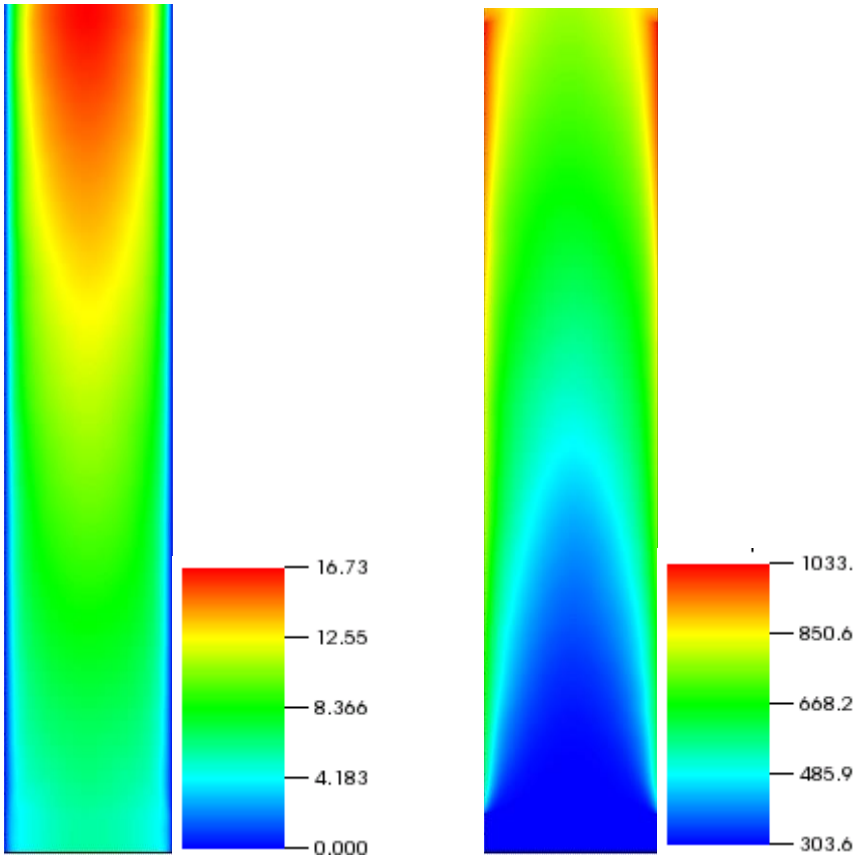

Figure 3-6. Time averaged fields on XZ-plane (Y=0) for Run-6; (a) Velocity (m/s) and (b) Temperature (K)

Table 3-3. Comparison of Re and Nu at inlet and outlet of DTHT test section using STAR-CCM+ RSM

RUN	INLET		OUTLET		%DTHT
	Re	Nu	Re	Nu	$(Nu_{Inlet} - Nu_{Outlet})/Nu_{Inlet} \times 100$
4	8927	13.1	4029	6.2	52.67
6	6716	21.9	3385	10.76	50.86
7	6667	21.9	3633	11.38	48.03

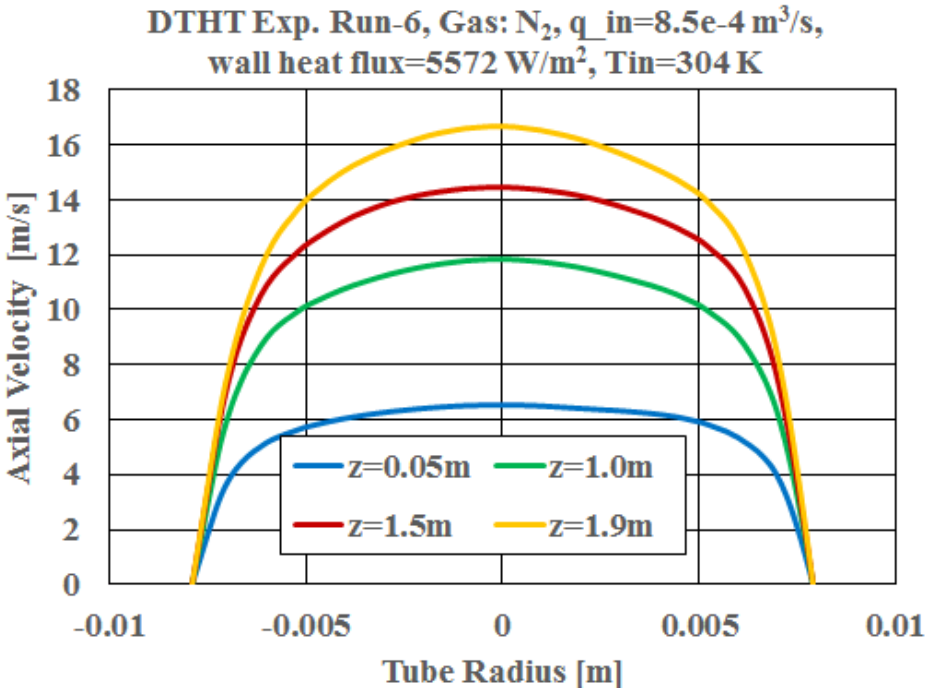

Figure 3-7. Nek5000 Axial velocity profiles across radial direction at various axial locations for Run-6.

As seen in Figure 3-7, velocity profiles were tending towards laminarization (parabolic nature) in the outlet region (~1.9 m). It is evident that the acceleration effects were dominant due to rapid change of velocities in the core region. In Table 3-3, the reduced heat transfer coefficients (Nu) were mainly due to the laminerized velocity profile towards an outlet (z=1.9m). For Run-6, 50% DTHT was calculated at the outlet when compared to the inlet. Similar observations were found for other runs (Run-4 and Run-7).

As seen in Figure 3-8(a), the calculated wall temperatures were in good agreement with the measured data, except at outlet. In Figure 3-8(b), only simulation data was shown due to unavailable measured data for Run-4. For Run-4 and Run-7, the predicted DTHT was similar to Run-6 (Table 3-3).

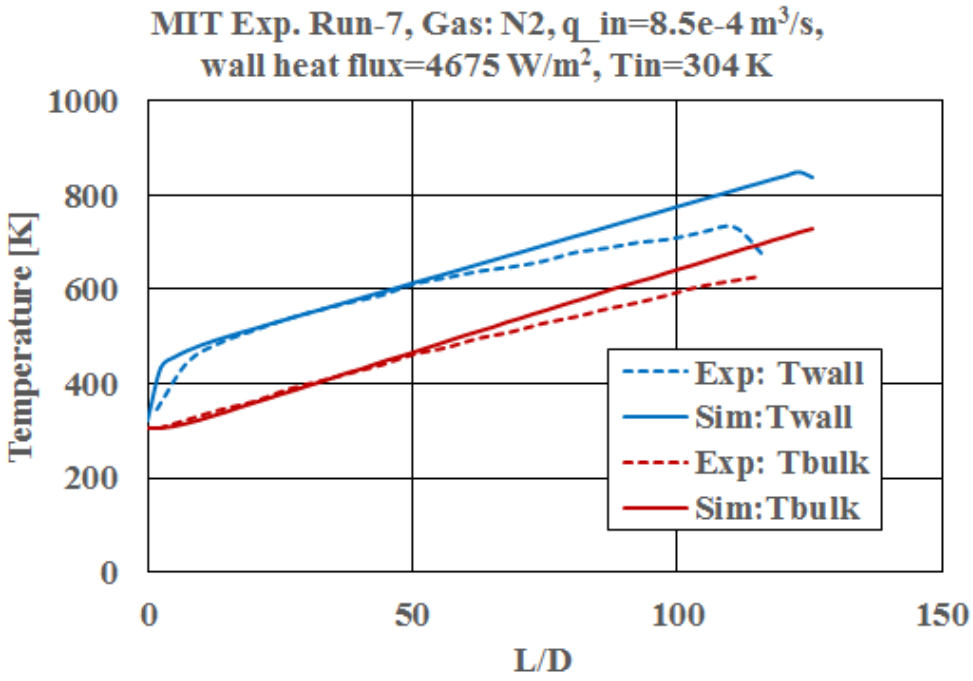

(a)

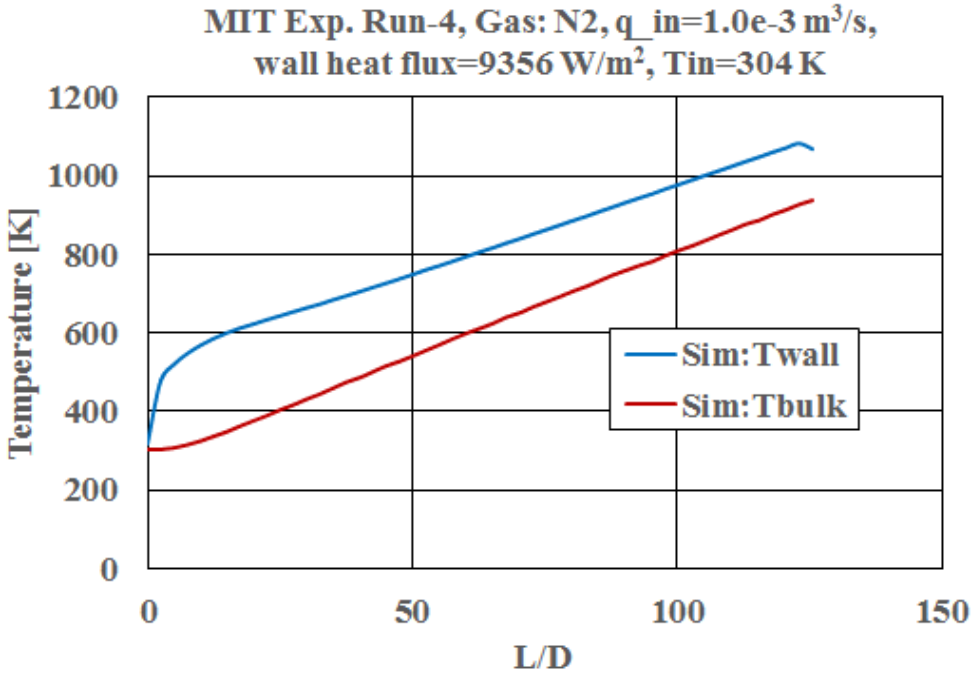

(b)

Figure 3-8. Comparison of wall and bulk temperatures along the axial direction of the test section using STAR-CCM+ RSM for (a) Run-7 and (b) Run-4.

3.6 Conclusions

3D CFD models were verified and validated with data of MIT DTHT benchmark test using both Nek5000 and STAR-CCM+ RSM. For Run-6, good agreement was observed between both simulated and experiments for both wall and bulk temperatures using Nek5000. In contrast, STAR-CCM+ results were underpredicted for Run-6 due to higher turbulence in the wall region. Further, only STAR-CCM+ results were performed for Run-4 and Run-7. In these runs, the predicted DTHT was over 48% at outlet when compared to inlet heat transfer values.

4 FUTURE WORK

Future work will include analyzing the modular HTGR domain for PCC event and developing the heat transfer correlations for natural circulation regime using Nek5000. In the PCC event, the Reynolds numbers can approach as low as ~500 during the development of a natural circulation flow from a forced circulation flow. The high-fidelity CFD tool can help to guide the low order models to accomplish the plant level simulations, efficiently and accurately. This effort includes collecting heat transfer correlations from literature and verifying with the Nek5000 results for various Reynolds flows (50 to 2000) and wall heat fluxes (1000 to 20000 W/m^2). Further, the Nek5000 simulations can be performed to investigate the influence of wall heated coolant channel flow on jet or plume mixing in an upper plenum. These simulations can be used as a numerical benchmark test for verification of ongoing developments in lower-order codes such as Pronghorn.

The final goal of this project is to build an integrated tool collaborating with Idaho National Laboratory (INL), this effort aims for the development of a computationally efficient capability that attempts to predict flow and heat transfer in the core and plena during the transient events. To achieve this, we plan to integrate 2-D or 3-D coarse-mesh engineering-scale simulation tools like PRONGHORN (for the core) [14] and 1-D system analysis code SAM (for the primary loop and the plant) [15] along with 3-D tools like Nek5000 (for the plena) [5].

ACKNOWLEDGMENTS

This work was funded by the U.S Department of Energy, Office of Nuclear Energy, Nuclear Energy Advanced Modeling and Simulation (NEAMS) program, under Argonne contract DE-AC02-06CH11357.

We gratefully acknowledge the computing resources provided on Bebop, a high-performance computing cluster operated by the Laboratory Computing Resource Center at Argonne National Laboratory.

Special thanks to Alex Obabko (MCS) and Richard Schultz (ISU) for their support and valuable suggestions throughout this work.

5 REFERENCES

1. G.E. Mccreery et al., "Scaled experimental modeling of VHTR plenum flows," *15th International Conference on Nuclear Engineering* (ICONE 15), Japan. (2007).
2. J.N. Reyes et al., "Scaling analysis for the high temperature Gas Reactor Test Section (GRTS)," *Nuclear Engineering and Design*, **240**(2): p. 397-404 (2010).
3. P. Fisher et al., "Petascale algorithms for reactor hydrodynamics," *J. Phys. Conf. Series,* (2008).
4. STAR-CCM+-v9.06.011, User Guide (2014).
5. R.R. Schultz et al., "Identification and characterization of thermal fluid phenomena associated with selected operating/accident scenarios in modular high temperature gas-cooled reactors," Idaho National Laboratory, INL/EXT-17-43218 (2017).
6. Y. Hassan, "Experimental and CFD studies of coolant flow mixing within scaled models of the upper and lower plenums of NGNP gas-cooled reactors," *NEUP Project No.* 12-3759, 2016.
7. A. Alfafy et al., "Texas A&M university jet impingement benchmark experiment," un-published (2017).
8. J.I. Lee et al., "Studies of the deteriorated turbulent heat transfer regime for the gas-cooled fast reactor decay heat removal system", *International Conference on Nuclear Engineering ICONE14 '06*, Paper 89826, Miami, Florida USA, July 17-20, 2006.
9. J.I. Lee et al., "Transitional flow from laminar to turbulent mixed convection in a heated vertical pipe", *International Congress on Advances in Nuclear Power Plants ICAPP '05*, Paper 5320, Seoul, Korea, May 15-19, 2005.
10. J.I. Lee et al., "Studies of the deteriorated turbulent heat transfer regime for the gas-cooled fast reactor decay heat removal system," *Nuclear Engineering and Design*, **237**(10): p. 1033-1045 (2007).
11. J.I. Lee et al., "Deteriorated turbulent heat transfer of gas up-flow in a circular tube: experimental data," *International Journal of Heat and Mass Transfer*, 51(1-2): p. 3259-3266 (2008).
12. J.I. Lee et al., "Deteriorated turbulent heat transfer of gas up-flow in a circular tube: heat transfer correlations," International Journal of Heat and Mass Transfer, 51(1-2): p. 5318-5326 (2008).

13. L.M. Kyle, “Experimental design and flow visualization for the upper plenum of a very high temperature gas cooled for computer fluid dynamics validation,” *Master Thesis*, Texas A&M university, (2014).
14. Idaho National Laboratory, PRONGHORN Manual, (2017).
15. R. Hu, “SAM theory manual”. Argonne National Laboratory, ANL/NE-17/4 (2017).

Nuclear Science and Engineering Division
Argonne National Laboratory
9700 South Cass Avenue, Bldg. 208
Argonne, IL 60439

www.anl.gov